Calculation of Zn-Doped Y Ceramics by the Electron-Correlated Embedded-Cluster Method

I. G. KAPLAN,[1,2] J. SOULLARD[2]

[1]*Instituto de Investigaciones en Materiales, UNAM, Apdo. Postal 70-360, 04510 México, D.F., Mexico*
[2]*Instituto de Física, UNAM, Apdo. Postal 20364, 01000 México, D.F., Mexico*

Received 26 January 2000; revised 27 March 2000; accepted 14 June 2000

ABSTRACT: An approach, where the embedded-cluster method (ECM) is applied in the frame of the Gaussian program to calculate the local electronic structure of crystals at the electron correlation level is presented. This approach is applied to a ground-state electronic structure calculation of the pure and Zn-doped Y123 ceramics at the second-order Møller–Plesset (MP2) correlation level (the ECM-MP2 approach). This allows to study the influence of the Zn doping on the charge distribution and the hole symmetry on the Cu and O ions obtained in the natural bond orbital (NBO) population analysis at the MP2 level. The possible mechanisms of the degradation of superconductivity in the Zn-doped Y ceramics are discussed. Int J Quantum Chem 80: 320–326, 2000

Key words: embedded-cluster method; electron correlation; Zn-doped yttrium ceramics; high T_c superconductivity

Introduction

In spite of the activity in experimental and theoretical studies of high T_c superconductivity (HTSC), the mechanism of this phenomenon remains obscure. The numerous theories are based on some model assumptions and usually contain parameters, however, as exceptions two recent studies have to be cited [1, 2]. For creating a microscopic theory of the HTSC phenomenon further comparative experimental and theoretical studies of SC and non-SC ceramics are needed.

Shortly after the discovery of the HTSC, it was revealed that the doping of the Zn or Ni atoms destroys the superconductivity [3, 4]. At present, their destructive action is very well established [5–7]. It is known, for instance, that the substitution of 8–10% Cu by Zn results in the full suppression of superconductivity. The Zn is a nonmagnetic atom; the Ni has a magnetic moment. The comparative study of their action can help to elucidate the na-

Correspondence to: I. G. Kaplan.
Contract grant sponsor: DGAPA-UNAM.
Contract grant number: IN108697.
Contract grant sponsor: CONACyT (Mexico).
Contract grant number: 32227E.

ture of pairing or, at least, to exclude some pairing mechanisms [8].

The main problem in the material science is to find the connection

Physical properties ↔ chemical structure.

For finding this relation in the HTSC ceramics, we have, at least, to know the detailed electronic structure and the changes induced by impurities that suppress T_c. To reveal the peculiarities in the electronic structure of doped ceramics, the band calculations have to be supplemented by calculations of local electronic structure. The most appropriate approach for this is the embedded-cluster method (ECM) [9, 10]. This method includes two parts:

1. A method used for a quantum mechanical calculation of cluster. In our case, the many-electron system associated with the embedded finite cluster is treated by the restricted or unrestricted Hartree–Fock self-consistent field method. In order to take into account the electronic correlation, the second-order Møller–Plesset perturbation theory (MP2) is used. So, our approach can be denoted as the ECM-MP2.
2. An embedded scheme to couple the cluster to its environment which should represent an infinite crystal. This scheme will be described in the next section.

A general discussion of the application of the ECM to Y ceramics and the relevant literature are given in Refs. [11, 12]. There we elaborated on the version of the ECM that allows to take into account the electron correlation effects in the frame of the Gaussian package.

Our approach differs from that of Gupta and Gupta [13, 14] who studied recently the Zn and Ni impurity effects in $YBa_2Cu_3O_7$ using a recurrent tight-binding approximation. Their approach allows to employ a cluster with more than 10,000 atoms but does not take into account the electron correlation. The latter plays an extremely important role in copper–oxide ceramics [15]. As shown in our previous calculations of Y ceramics [11, 12], the effects of the electron correlation at the MP2 level essentially change the charge and spin distributions (e.g., the magnitude of the electron correlated charge on copper ions decreases by a factor 1.5 in comparison with the Hartree–Fock charges).

In the present work, the local electronic structure of undoped and Zn-doped Y123 ceramics is calculated by means of the ECM-MP2 approach. As shown by X-ray absorption fine-structure (XAFS) experiments [16], the Zn atoms at small concentration occupy the Cu(2) plane sites of $YBa_2Cu_3O_7$ crystals. Thus, in order to study the effects of the substitution of Cu by Zn, it is sufficient to consider clusters located in the CuO_2 plane. We performed the calculation of two planar clusters—$[Cu_4O_{12}]^{-12}$ and $[Cu_2Zn_2O_{12}]^{-12}$. The cluster charge -12 is obtained with the atomic charges of Ref. [17]. The comparison of the results allows to obtain the variation in the charge distribution, as well as in the hole symmetry on the Cu and O ions, caused by the Zn doping.

Methodology

The clusters are embedded into a finite array of charges that simulates the Madelung potential of the infinite crystal lattice. This is achieved by means of a procedure originally proposed by Kelires and Das [18]. Its principle consists in adjusting the charges of the outermost ions of the array in order to provide the correct value of the Madelung potential on each cluster site as well as the electrical neutrality of the final set of charges. This is realized by solving a system of $n + 1$ linear equations if the potential on n sites has to be reproduced (one equation is left to express the electrical neutrality) [19].

When the cluster is small and presents the same point group as the crystalline structure, it was found that the reproduction of the Madelung potential on the cluster sites with distinct values of the potential ($k_{\min}$ denotes the number of these sites) is sufficient to reproduce the Madelung potential on all cluster sites [11, 12]. However, for larger clusters which symmetry is lower than that of the crystalline structure (D_{2h} for $YBa_2Cu_3O_7$), the number of adjusted cluster sites must be greater than $k_{\min}$ in order to obtain a homogeneous reproduction of the Madelung potential. It will depend indeed on the number of shells that can be defined on the external surface of the cluster. In the case of the clusters studied in the present work (three different sites and C_{2v} symmetry), a system of 11 linear equations was needed to obtain satisfactory results (precision better than 2×10^{-5} on all cluster sites).

Generally, the charges of cluster ions obtained after a calculation at the MP2 level differ from the initial ones taken for the background ions, and in the case where the cluster does not coincide with the unit cell, this causes that the unit cell, associ-

ated with new ionic charges, is not neutral. In order to get consistency between cluster and background charges, a series of calculations has been performed where the charges obtained as a result of a calculation are taken as background charges for the next calculation; at each step, the ionic charges are modified in order to assure the electrical neutrality of the unit cell and to preserve the initial cluster charge [12].

The clusters studied by means of the ECM have to be representative of the crystal and adequate to the problem that has to be solved. As noted in the Introduction, at small concentration, the Zn atoms are located in the CuO_2 planes, and this justifies the choice of Cu_nO_m planar clusters. The cluster size is also very important and must be chosen so as to minimize the "boundary effects." These effects occur at the interface cluster–background charges where the ion charges on the external surface of the cluster are different from that of the equivalent ions inside the cluster.

The ab initio quantum mechanical calculations of the cluster were done using the Gaussian 94 program [20]. The finite array of background charges was introduced as solvent charges using the CHARGE keyword of the program. The triply split valence 6-311G basis set was used in the restricted Hartree–Fock (RHF) and MP2 calculations. We did not used pseudopotentials; all core electrons were directly included in the ab initio calculations. To calculate charge distribution we used the Mulliken population analysis along with the natural bond orbital (NBO) option provided by the program. For the determination of the symmetry of holes on cluster atoms, the NBO population data were used.

The flowchart corresponding to the complete embedding procedure is shown in Figure 1.

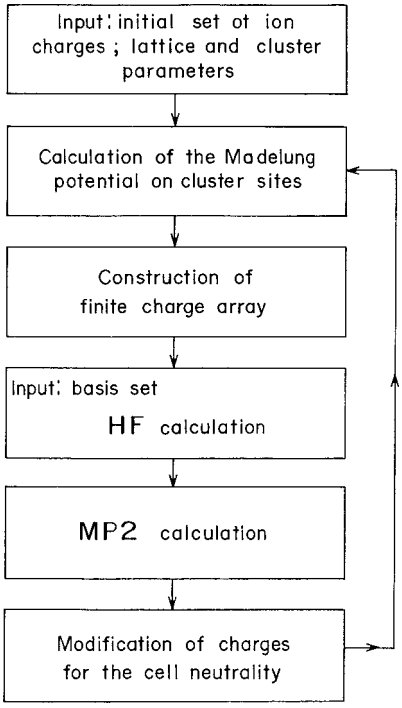

FIGURE 1. Iteration cycle in the self-consistent charge calculation.

Results and Discussion

The influence of the crystal field on the charge distribution calculated at the MP2 level was at first tested for both clusters. In Table I, we present the comparative calculation of the isolated clusters and the clusters embedded into the Madelung potential of the crystal. According to the data presented, the influence of the crystal surrounding is very strong: the Cu2 charge increases by the factor 3–3.4, the oxygen charge by the factor 1.6–1.7, and the Zn charge undergoes a smaller increase, 1.2. This indicates that the results obtained for the isolated cluster cannot be extended to the local crystal structure.

In Figure 2, we present the charges on atoms and bonds obtained from the condensed atoms charge matrix calculated at the MP2 level. The charges on bonds are given as fractions of the electron charge, so, they are negative. Due to the boundary effects, the charges on the outermost oxygen ions are different from those on the equivalent oxygens inside the cluster. It may be asked whether the clusters chosen in our approach are representative of the crystal

TABLE I
Influence of the Madelung potential on the atomic (Mulliken) charges in the cluster at the MP2 level (in a.u.).

	Isolated cluster	Cluster in crystal
Cu_4O_{12}		
Cu2	+0.44	+1.33
O2	−0.87	−1.39
O3	−0.84	−1.40
$Cu_2Zn_2O_{12}$		
Zn	+1.31	+1.62
Cu2	+0.40	+1.36
O2	−0.90	−1.58
O3	−0.87	−1.60

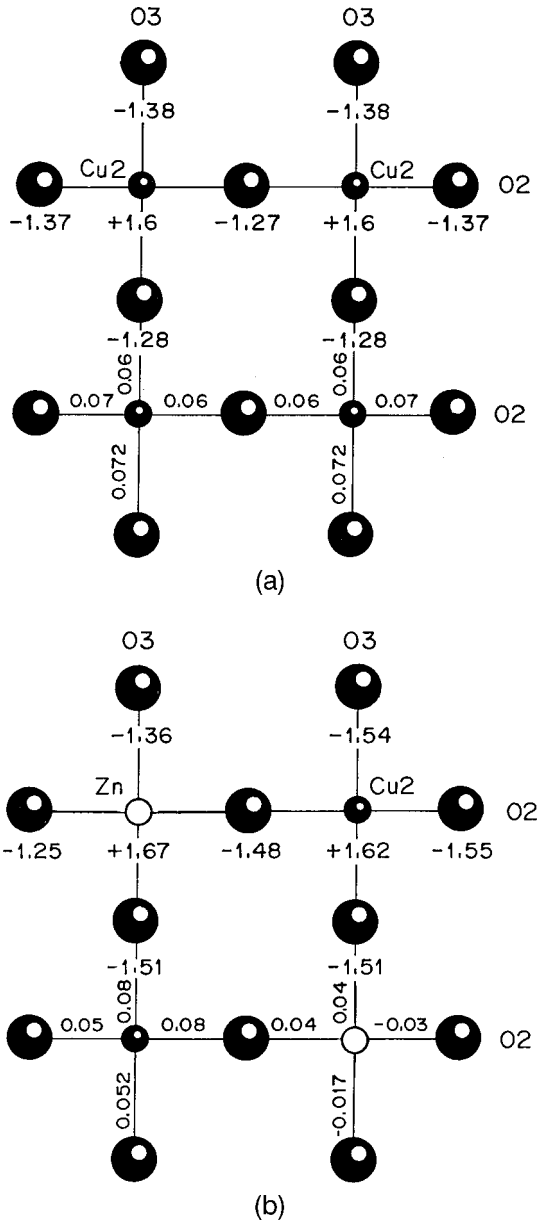

FIGURE 2. Charge distribution obtained at the MP2 level.

and adequate to study the effects of impurity doping on the electronic structure of $YBa_2Cu_3O_7$. In our case, the cluster Cu_4O_{12} is considered as the minimum cluster to obtain reliable results if the charge of inner oxygen ions only are taken into account (the function of external oxygens being essentially to reproduce the correct environment of coppers). Therefore, in Table II, where we present the valence orbital population and charges on atoms obtained from the NBO analysis, the inner oxygen ions are only considered. In the valence bond population of

TABLE II

Self-consistent charge distribution at the MP2 level for the clusters Cu_4O_{12} and $Cu_2Zn_2O_{12}$ obtained from the NBO population analysis.

	Charges on atoms	Valence orbital population
Cu_4O_{12}		
Cu2	+1.37	$4s^{0.29}3d^{9.26}$
O2	−1.28	$2s^{1.93}2p^{5.42}$
O3	−1.28	$2s^{1.93}2p^{5.42}$
Cu_2ZnO_{12}		
Zn	+1.68	$4s^{0.26}3d^{9.97}$
Cu2	+1.41	$4s^{0.28}3d^{9.22}$
O2	−1.48	$2s^{1.93}2p^{5.62}$
O3	−1.51	$2s^{1.94}2p^{5.65}$

Table II, the small populated excited orbitals are not included, but their population is taken into account in the values of atomic charges. The comparison of the data of Tables I and II shows that the difference between the Mulliken charges and that obtained from the more precise NBO analysis is not large on the Cu atoms, 0.04–0.05*e*, and twice as much on the O atoms, 0.10–0.12*e*.

According to the valence orbital population in the crystal (Table II), both the 3*d* and 4*s* copper electrons are involved in the interaction with the nearest oxygen neighbors. The interaction Cu(3*d*)–O(2*p*) leads to an antibonding state [21, 22], while the interaction Cu(4*s*)–O(2*p*) stabilizes the crystal forming a covalent bond with an electron density equal to 0.06*e* (Fig. 2). In Zn-doped ceramics, the Cu–O bond nearest to the Zn becomes even more covalent, the electron density on the bond increases to 0.08*e*. The electron density on the Zn–O bond decreases (compared with the Cu–O bond) to 0.04*e*, but it still has the covalent nature. The 4*s* electrons of Zn are to a great extent involved with crystal interactions. The population $4s^2$ (in the Zn atom) becomes $4s^{0.26}$ (in the crystal). On the other hand, the *d* electrons of Zn do not participate in the binding: the 3*d* subshell of Zn is almost filled, $3d^{9.97}$. This means that the antibonding state Cu(3*d*)–O(2*p*) vanishes in the regions where the Cu is substituted by Zn.

The substitution of Cu by Zn produces an additional electron in the crystal. This negative charge distributes mostly on the neighboring O atoms and partly on the Zn–O bonds. As a result, the concentration of holes in the vicinity of the Zn impurity decreases. According to Table II, the reduction of

the hole density on the CuO_2 units, adjacent to the Zn, is 0.39*e*. There is a small increase, +0.04*e*, of the positive charge on the Cu2 and a large charge variation on the nearest oxygens: −0.20*e* on O2 and −0.23*e* on O3. This charge variation increases the O(2*p*) population. Note the excess of positive charge of +0.31*e* on the Zn site (with respect to the Cu site of undoped ceramics), in spite of the additional 4*s* electron inserted with the Zn impurity.

Thus, as in the tight-binding model calculations [13, 14], our results indicate that the Zn doping leads to a delocalized hole nonuniformity along the Zn–O–Cu directions. This extended inhomogeneity in the hole distribution in the vicinity of the Zn sites can enhance the carrier scattering cross section and lead to the destruction of superconductivity. The study of the Zn substitution effects on the normal-state charge transport in $YBa_2Cu_3O_7$ ceramics revealed a large scattering cross section of the Zn impurities [23]. According to Fukuzumi et al. [6], the primary effect of Zn doping is to produce a large residual resistivity as a potential scattering center in the unitarity limit.

For creating the theory of the HTSC, it is important to know the symmetry of holes that are the charge carriers of superconducting ceramics. In the early band calculations [24, 25], the 2*pσ* symmetry of the holes on oxygen ions was obtained. Later in the generalized bond calculations [26], without taking into account the crystal field, the 2*pπ* symmetry of the holes on oxygen ions was reported. In our recent studies [11, 12] of $YBa_2Cu_3O_7$ ceramics by the ECM-MP2 approach, we obtained the 2*pσ* symmetry of the holes on the oxygens in the CuO_2 plane. We confirm these results in the present calculations; see Figure 3(a). This information was extracted from the NBO analysis data after calculation of the $[Cu_4O_{12}]^{-12}$ embedded cluster at the MP2 level.

It is interesting to note that a picture similar to that presented in Figure 3(a) was proposed by Zhang and Rice [27] without any rigorous treatment. They assume that on the CuO_2 planes of superconducting ceramics the hybridization of 3*d*(Cu) and 2*p*(O) electrons is realized and all spins are paired (the so-called Zhang–Rice singlet). Now their hypothesis is substantiated by our ECM-MP2 calculations. The results about the hole symmetry presented in Figure 3(a) are in good agreement with the nuclear magnetic resonance (NMR) experiments [28, 29] and the recent X-ray absorption spectroscopy studies [30].

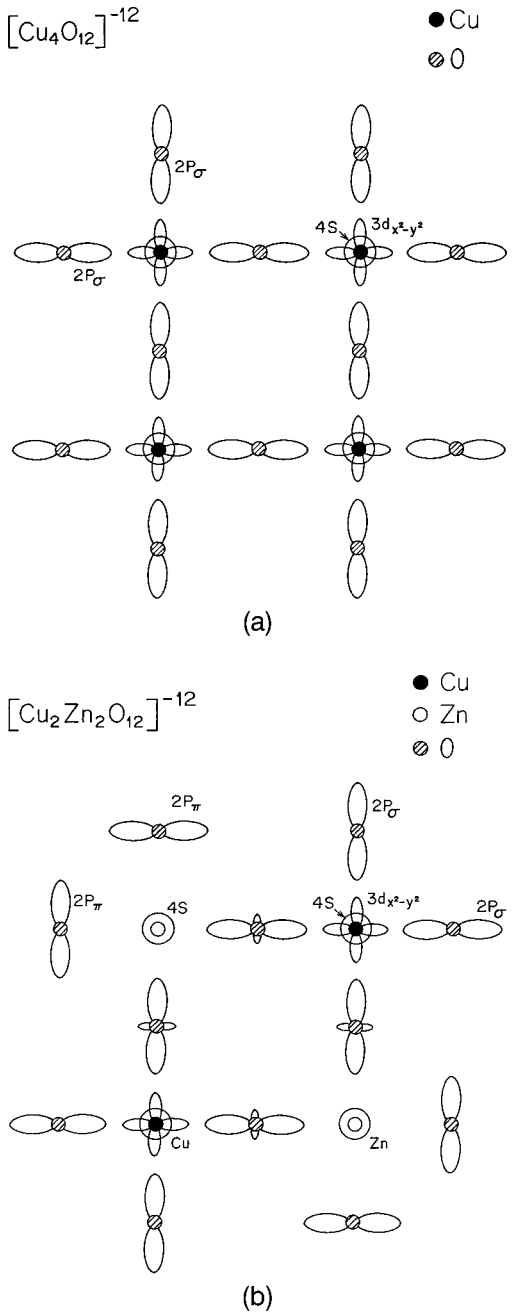

FIGURE 3. Symmetry of holes obtained from the NBO population analysis at the MP2 level.

The NBO analysis allows to obtain additional information. The hole on the Cu2 has, in addition to the anisotropic $3d_{x^2-y^2}$ symmetry, an isotropic component from the 4*s* orbital, which is not small. The absolute contributions of each component are the following:

$$0.66\ 3d_{x^2-y^2} + 0.71\ 4s.$$

In the case of Zn-doped $YBa_2Cu_3O_7$ ceramics, the symmetry of the holes obtained from the NBO population analysis is presented in the Figure 3(b). It is very sensitive to the surrounding. This is why the holes on the outermost oxygens have a symmetry different from that of equivalent inner oxygens. We put into consideration only the latter. The calculation of a more representative cluster, Cu_8O_{24}, is now in progress in our group.

As follows from Figure 3(b), at oxygen sites close to the Zn impurity, the pure $2p\sigma$ symmetry in the undoped material is modified and shows a $2p\pi$ contribution. The NBO analysis data give the following superposition of symmetries of holes on oxygens adjacent to the Zn:

$$0.28\ 2p\sigma + 0.06\ 2p\pi\ (\text{in plane}) + 0.04\ 2p\pi\ (\perp \text{plane}).$$

This change of symmetry can hinder the hole–pair formation on oxygens in the vicinity of the Zn impurity.

The hole on Zn has the isotropic $4s$ symmetry. The symmetry of the hole on the adjacent Cu2 is

$$0.71\ 3d_{x^2-y^2} + 0.74\ 4s.$$

It is practically not modified in comparison with the pure ceramics.

As measured in Ref. [31], the coherence length of Zn- and Ni-doped Y123 single crystals increases upon impurity doping. This indicates that impurities act as pair breakers. The change of the hole symmetry on the O atoms adjacent to the Zn, which is revealed in our study, can be considered as a possible mechanism responsible for the pair breaking. Thus, this result is in agreement with the experimental observation [31].

Conclusions

The ECM-MP2 approach developed in our previous works [10, 11] is generalized to clusters with arbitrary symmetry. It allows to make calculations at the electron correlation level provided by the Gaussian package. One of advantages of this approach is the possibility to use the rather precise NBO population analysis at the electron correlation level.

The application of our approach to the comparative calculation of the local electronic structure of pure and Zn-doped ceramics reveals three qualitative changes that can lead to the destruction of superconductivity in the Zn-doped Y ceramics:

1. The reduction in the amount $0.39e$ of the hole density on the CuO_2 units adjacent to Zn. This leads to a hole nonuniformity along the Zn–O–Cu directions and can enhance the carrier scattering cross section.
2. On the contrary to the Cu ions, the d subshell of Zn does not practically participate in the crystal interactions. This leads to the destruction of the Cu($3d$)–O($2p$) antibonding band in the vicinity of the Zn impurity.
3. According to the NBO population analysis at the MP2 level, the pure $2p\sigma$ symmetry on oxygen ions in the CuO_2 planes in undoped Y ceramics is changed. On the oxygens adjacent to the Zn, the symmetry of holes presents a contribution from the $2p\pi$ symmetry greater than 25%. This change of symmetry can hinder the hole–hole formation.

The calculation of more representative Zn-doped clusters is now in progress.

ACKNOWLEDGMENTS

This study was partly supported by grants from DGAPA-UNAM IN108697 and CONACyT (Mexico) 32227E. We thank the staff of DGSCA-UNAM for the allotment of the facilities of their supercomputers.

References

1. Alexandrov, A. S.; Kabanov, V. V. Phys Rev B 1999, 59, 13628–13631.
2. Abrikosov, A. A. Int J Mod Phys B 1999, 13, 3405–3417.
3. Mandal, P.; Poddar, A.; Choudhury, P.; Das, A. N.; Ghosh, B. J Phys C 1987, 20, L953–L957.
4. Jayaram, B.; Agarwal, S. K.; Navasimha Rao, C. V.; Narlicar, A. Y. Phys Rev B 1988, 38, 2903–2905.
5. Zagaulaev, S.; Monod, P.; Jegoudez, J. Phys Rev B 1995, 52, 10474–10487.
6. Fukuzumi, Y.; Mizuhashi, K.; Takenaka, K.; Uchida, S. Phys Rev Lett 1996, 76, 684–687.
7. Ruvalds, J. Supercond Sci Technol 1996, 9, 905.
8. Sigrist, M.; Ueda, K. Rev Mod Phys 1991, 63, 239–312.
9. Catlow, C. R. A.; Mackrodt, W. C., Eds.; Computer Simulation of Solids; Springer: Berlin, 1982.
10. Vail, J. M.; Pandey, H.; Kunz, A. B. Rev Solid State Sci 1991, 5, 241.
11. Kaplan, I. G.; Soullard, J.; Hernández-Cobos, J.; Pandey, R. J Phys Conden Mat 1999, 11, 1049–1058.
12. Kaplan, I. G.; Hernández-Cobos, J.; Soullard, J. Prog Theor Chem Phys B 2000, 1, 145–161.
13. Gupta, R. P.; Gupta, M. Physica C 1998, 305, 179–184.

14. Gupta, R. P.; Gupta, M. Phys Rev B 1999, 49, 3381–3384.
15. Brenig, W. Phys Rev 1995, 251, 153–215.
16. Bridge, F.; Li, G.; Boyce, J. B.; Claeson, T. Phys Rev B 1993, 48, 1266–1271.
17. Gupta, R. P.; Gupta, M. Solid State Commun 1988, 67, 129–133.
18. Kelires, P. C.; Das, T. P. Hyperfine Interact 1987, 34, 285.
19. Shrinivas, S. Ph.D. Thesis, SUNY, Albany, 1995.
20. Frich, M. J.; Trucks, G. W.; Schlegel, H. B.; Gill, P. M. W.; Johnson, B. G.; Robb, M. A.; Keith, T.; Petersson, G. A.; Montgomery, J. A.; Raghavachari, K.; Al-Laham, M. A.; Zakrzewski, V. G.; Ortiz, J. V.; Foresman, J. B.; Cioslowski, J.; Stefanov, B. B.; Nanayakkara, A.; Challacombe, M.; Peng, C. Y.; Ayala, P. Y.; Chen, W.; Wong, M. W.; Andres, J. L.; Replogle, E. S.; Gomperts, R.; Martin, R. L.; Fox, D. J.; Binkley, J. S.; Defrees, D. J.; Baker, J.; Stewart, J. P.; Head-Gordon, M.; Gonzales, C.; Pople, J. A. Gaussian 94, Revision C.3; Gaussian: Pittsburgh, 1995.
21. Novikov, D. L.; Ryzhkov, M. V.; Gubanov, V. A. Zh Strukt Khim 1989, 30, 17–26.
22. Vaisberg, B. S.; Kaplan, I. G.; Smutny, N. V. Superconductivity 1992, 5, 975–982.
23. Chien, T. R.; Wang, Z. Z.; Ong, N. P. Phys Rev Lett 1991, 67, 2088–2091.
24. Mattheiss, L. F. Phys Rev Lett 1987, 58, 1028–1031.
25. Yu, J.; Freeman, A. F.; Hu, J. H. Phys Rev Lett 1987, 58, 1035–1038.
26. Guo, Y.; Langlois, Y. M.; Goddard III, W. A. Science 1988, 239, 896–899.
27. Zhang, F. S.; Rice, T. M. Phys Rev B 1988, 37, 3759–3761.
28. Alloul, H.; Ohno, T.; Mendels, P. Phys Rev Lett 1989, 63, 1700–1703.
29. Takigawa, M.; Hammel, P. C.; Heffner, R. H.; Fisk, Z.; Smith, J. L.; Schwarz, R. B. Phys Rev B 1989, 39, 300–303.
30. Nücker, N.; Pellegrin, E.; Schweiss, P.; Fink, J.; Molodtsov, S. L.; Simmons, C. T.; Kaindl, G.; Frentrup, W.; Erb, A.; Müller-Vogt, G. Phys Rev B 1995, 51, 8529–8542.
31. Tomimoto, K.; Terasaki, I.; Rykov, A. I.; Mimura, T.; Tajima, S. Phys Rev B 1999, 60, 114–117.